Journal of Colloid and Interface Science 615 (2022) 265–272

Contents lists available at ScienceDirect

Journal of Colloid and Interface Science

journal homepage: www.elsevier.com/locate/jcis

pH-Controlled assembly of polyelectrolyte layers on silica nanoparticles in concentrated suspension

Krzysztof Kolman [a,d,*], Giovanna Poggi [b], Michele Baglioni [b,1], David Chelazzi [b], Piero Baglioni [b,1], Michael Persson [a,c], Krister Holmberg [a], Romain Bordes [a,*]

[a] Department of Chemistry and Chemical Engineering, Chalmers University of Technology, Göteborg, Sweden
[b] Department of Chemistry and CSGI, University of Florence, Florence, Italy
[c] Nouryon, Bohus, Sweden
[d] Present address: Nouryon Surface Chemistry, Stenungsund, Sweden

GRAPHICAL ABSTRACT

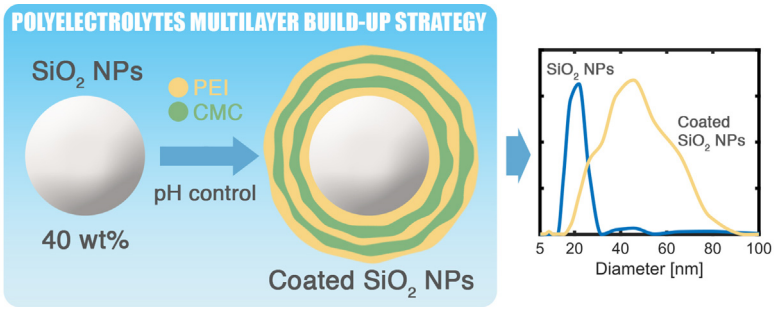

ARTICLE INFO

Article history:
Received 24 September 2021
Revised 18 January 2022
Accepted 19 January 2022
Available online 22 January 2022

Keywords:
Silica
Nanoparticle
Polyelectrolyte
Polyelectrolyte layers
Controlled assembly
Adsorption
Aggregation
Concentrated suspension

ABSTRACT

Hypothesis: Preparation of suspensions of nanoparticles (>1 wt%) coated with a polyelectrolyte multilayers is a challenging task because of the risk of flocculation when a polyelectrolyte is added to a suspension of oppositely charged nanoparticles. This situation can be avoided if the charge density of the polymers and particles is controlled during mixing so as to separate mixing and adsorption events.
Experiments: The cationic polyethylenimine (PEI) and the anionic carboxymethylcellulose (CMC) were used as weak polyelectrolytes. Polyelectrolyte multilayers build-up was conducted by reducing the charge of one of the components during the addition of the next component. Charge density was controlled by tuning pH. Analysis of the suspension of coated nanoparticles was done by means of dynamic light scattering, electrophoresis and small angle x-ray scattering measurements, while quartz crystal microbalance was used to study the build-up process on flat silica surfaces.
Findings: Charge density, controlled through pH, can be used as a tool to avoid flocculation during layer-by-layer deposition of polyelectrolytes on 20 nm silica particles at high concentration (~40 wt%). When added to silica at pH 3, PEI did not induce flocculation. Adsorption was triggered by raising the pH to 11, pH at which CMC could be added. The pH was then lowered to 3. The process was repeated, and up to five polyelectrolyte layers were deposited on concentrated silica nanoparticles while inducing minimal aggregation.

* Corresponding authors.
E-mail addresses: krzysztof.kolman@nouryon.com (K. Kolman), bordes@chalmers.se (R. Bordes).
[1] No kinship exists among these authors.

https://doi.org/10.1016/j.jcis.2022.01.120
0021-9797/

1. Introduction

Suspensions of nanoparticles are used in industrial applications of various kinds, e.g. ceramics and composites,[1,2] delivery systems,[3–5] coatings,[6,7] and in other important fields such as cultural heritage conservation.[8–13] An important reason behind their ubiquitous presence is the large specific surface area of the particles, provided by the colloidal nature of the suspension. Accordingly, continuous efforts have driven the development of industrially relevant strategies to modify the surface properties of nanoparticles.[14,15] One route is through layer-by-layer build-up of polyelectrolyte multilayers, where a polyelectrolyte (PE) is first deposited on an oppositely charged particle, leading to reversal of surface charge. Another PE, carrying the same charge as the starting surface, is then deposited, again leading to charge reversal. The procedure may be repeated several times, producing a thin multilayered film of PEs covering the dispersed particles. This layer-by-layer deposition technique, which was pioneered by Decher, has been applied to a wide range of dispersed particles.[16,17] Examples include gold,[18,19] latex,[20,21] clays, [22,23] titania nanosheets,[24] and silica particles.[25,26]

A frequently encountered problem with the layer-by-layer technique applied to colloidal dispersions is that of instability during deposition. When a polyelectrolyte solution is added to a suspension of particles of opposite charge, there is an intermediate stage where the particles are only partially covered by the added polyelectrolyte. Thus, oppositely charged patches may tend to attract each other, possibly leading to "patchwise flocculation". [21] The phenomenon is particularly pronounced at high concentration of particles and the most common way to avoid this problem is to work with dilute systems, preferably below 1 wt%. This way, once the layer-by-layer assembly is completed, the particles can be concentrated again by solvent evaporation. However, this is a severe limitation from an industrial perspective, where the removal of large volumes of solvent is undesirable. Ideally, one would like to be able to perform the layer-by-layer deposition starting from highly concentrated nanoparticle suspensions, so as to obtain a final concentration above a few wt%, avoiding a subse-

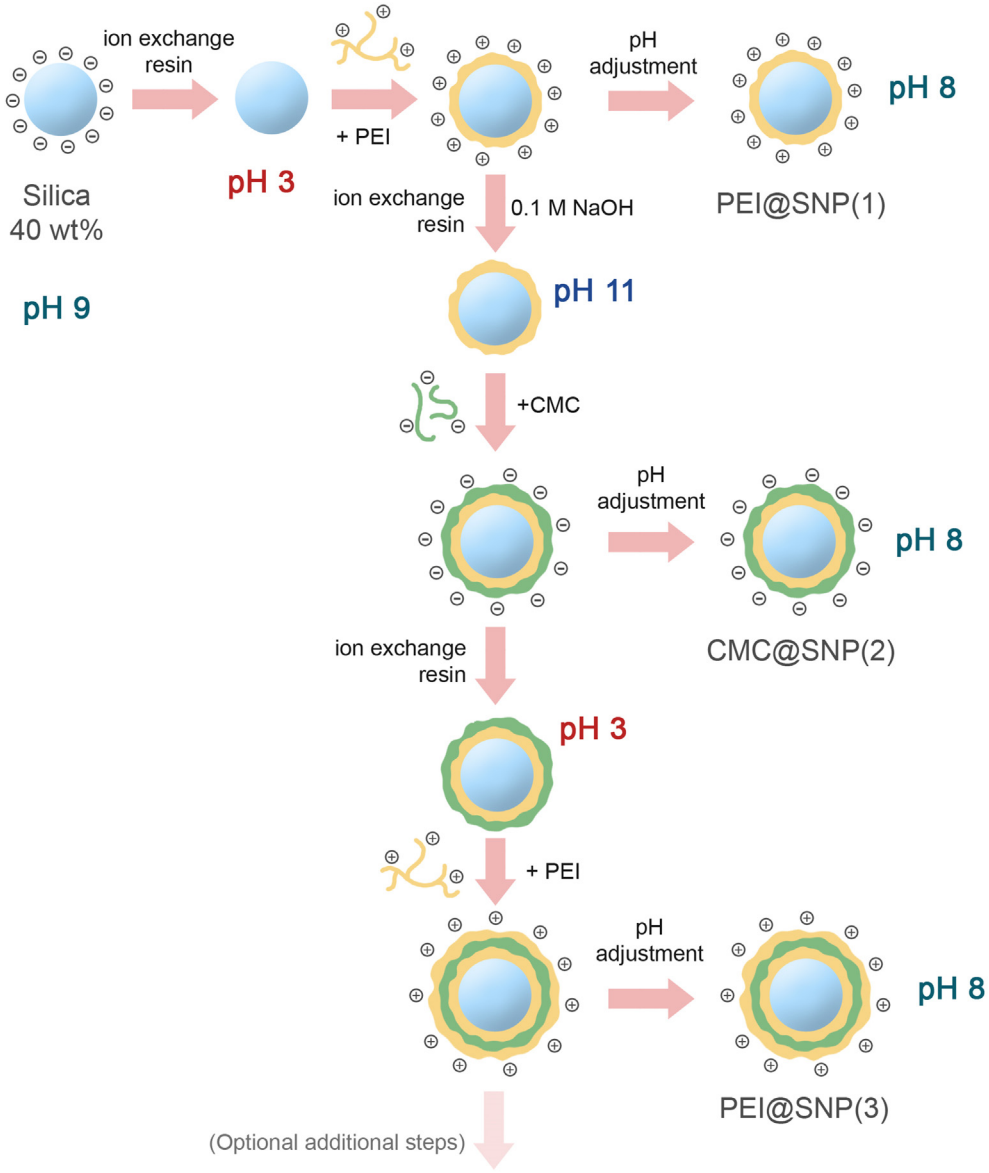

Fig. 1. Illustration of the PE multilayers (PEM) build-up strategy on a silica nanoparticle. At pH 3 silica is nearly neutral, as is CMC, while PEI has a low charge density at pH 11.

quent solvent removal step.[27] Such suspensions can be considered as high as compared to the ones reported in the literature. [28–32]

To this aim, we have developed a strategy based on controlling the charge density of the nanoparticles, silica in the present case (referred to as silica nanoparticles, SNP), and of two oppositely charged weak polyelectrolytes, namely polyethyleneimine (PEI) and carboxymethylcellulose (CMC), allowing the coating of silica with multiple alternated PEI and CMC layers, directly from highly concentrated suspensions (40 wt%). Following this approach, which is schematically illustrated in Fig. 1, we were able to deposit up to 5 PE layers without significant flocculation and reaching a final concentration above 4 wt%. The final coated SNP suspensions are named PEI@SNP(n) and CMC@SNP(n), indicating that there is a total of n PE layers and that PEI or CMC, respectively, is the last layer.

A combination of analytical techniques was used to obtain an indirect proof of the size and structure of the coated silica nanoparticles. Dynamic light scattering and small angle x-ray scattering provided complementary information about size changes of the particles upon PE layers addition. Further proof of the deposition of PE on a silica model surface was obtained from quartz crystal microbalance measurements.

2. Materials and methods

2.1. Materials

Silica nanoparticles sol (SNP) with tradename Levasil CS40-213 (former Bindzil 40/130) was provided by Nouryon (formerly AkzoNobel Pulp and Performance Chemicals). According to the producer, the surface area of these particles is 130 m^2/g which corresponds to a spherical diameter of 21 nm.[33] Polydispersity obtained from Cumulant fitting was around 0.05. The suspension has a pH of 9.1 (sodium ion stabilized), a silica concentration of 40 wt%, and a density of 1.3 g/ml.

Sodium carboxymethyl cellulose (CMC), with tradename Akucell AF0305, was provided by Nouryon (formerly AkzoNobel Pulp and Performance Chemicals). According to the producer, the degree of substitution of this polymer is 0.77 and the viscosity of 1 wt% solution is 12 mPa × s. The weight average molecular weight of CMC is 650000 g/mol (obtained by size exclusion chromatography). Branched polyethylenimine (PEI) with an average molecular weight of 25000 g/mol was purchased from Sigma-Aldrich. For pH adjustments, ion exchange resins Dowex Marathon A (OH^- form) and Dowex Marathon C (H^+ form), reagent grade sodium hydroxide and hydrochloric acid were used. All these chemicals were purchased from Sigma-Aldrich. The Dowex Marathon C resin was washed with ethanol and dried before use, while the other chemicals were used as received. The water used was purified with a Millipore purification system.

Particle charge density titrations were performed using solutions of 0.001 N poly(diallyldimethylammonium chloride) (polyDADMAC) and 0.001 N sodium poly(ethylene sulfonate) (PES-Na). Since charge density values were measured as a function of pH, the pH of titrants and samples was adjusted using sodium hydroxide or hydrochloric acid solutions.

2.2. Methods

2.2.1. Assembly of polyelectrolyte layers starting from high concentration of SNP (40 wt%)

The assembly of polyelectrolyte multilayers (PEM) on silica particles was performed as described in Fig. 1 using ion exchange resins to adjust the pH. Dowex Marathon C was used as the cation exchange resin, while Dowex Marathon A as the anion exchange resin. The anion exchange resin releases OH– ions, while consuming other anions that are present in the formulation. The cation exchange resin takes cations and releases H + ions. Resin beads are easily separated from the formulation after the ion exchange. Specifically, 1 ml of 40 wt% silica sol was first ion exchanged using the Marathon C resin to reach pH 3. In the next step PEI, a cationic polyelectrolyte, was adsorbed. Depending on the type of adsorbed layer, different amounts of PEI solution were used; the amounts were estimated using the particle charge detector titration (see Section 2.2.3). For adsorbing the first and intermediate PEI layers, 25 μl of 4.7 wt% solution at pH3 was added, while for the final layer 1 ml of the same solution (also at pH 3) was used. To adsorb CMC on particle coated with PEI, pH was raised to 11 using the Marathon A resin and a 0.1 M NaOH solution. Like for PEI adsorption, different amounts of CMC were applied. 42 μl and 1.68 ml of 2.8 wt% CMC solution at pH 11 were used for, respectively, the first intermediate and the final CMC layer. Using this adsorption strategy, silica/PE systems with up to 5 PE layers were obtained. The final pH of each sample was set to 8. The dry mass and composition of each sample (without water) are presented in Table S1.

2.2.2. Assembly of polyelectrolyte layers starting from low concentration SNP (0.5 wt%)

The assembly of polyelectrolyte multilayers (PEM) on silica particles was also performed at low concentration to be compared to the new approach here proposed. Samples were prepared as follow. First, 1 ml of 0.5 wt% silica dispersion in 10 mM NaCl at pH 3 was prepared. In the next step PEI was adsorbed. Depending on the type of adsorbed layer, different amounts of 0.06 wt% PEI solution in 10 mM NaCl were used. For PEI adsorbed as an intermediate layer, 25 μl of PEI solution at pH 3 was added, while for PEI adsorbed as a final layer, 1 ml of the same solution at pH 3 was used instead. To adsorb subsequent PE layers, pH was raised to 11 using the Marathon A resin and 0.1 M NaOH solution. In these conditions, CMC was adsorbed. Like for PEI adsorption, different amounts of CMC were applied. 25 μl and 1 ml of 0.06 wt% CMC solution in 10 mM NaCl at pH 11 were used for CMC adsorption as an intermediate and as a final polyelectrolyte layer, respectively. Using this adsorption strategy, the silica/PE systems with up to 2 PE layers were constructed. The final pH of each sample was set to 8.

2.2.3. Particle charge density determination

Particle charge density titrations of silica/PE complexes components were performed using a PCD 02 particle charge detector (Mütek) coupled with a Mettler DL21 titrator (Mettler Toledo). The technique allows the determination of the electrokinetic surface charge by measuring the streaming potential.[34,35] The anionic components were titrated with polyDADMAC solution and the cationic components were titrated with PES-Na solution.

2.2.4. Zeta potential determination

The zeta potential was measured using a ZetaPALS zeta potential analyzer (Brookhaven Instrument Corporation). The samples were diluted with 2 mM NaCl solution to a concentration of 0.05 wt% and filtered through 1.2 μm hydrophilic syringe filters. The zeta potential values were calculated according to the Smoluchowski theory.[36]

2.2.5. Dynamic light scattering (DLS)

The dynamic light scattering measurements were performed on a N4 Plus submicron particle analyzer (Beckman Coulter). The samples were diluted with Milli-Q water to concentration of 0.05 wt% and filtered through 1.2 μm hydrophilic syringe filter. The autocorrelation functions were collected at 90° for 300 s and analyzed

using a Kohlrausch–Williams–Watts (KWW) fitting function as well as the CONTIN inverse Laplace fitting routine.[37,38]

The KWW function formula is as follows:

$$g_1(t) = \alpha exp\left(\left(-\frac{t}{\tau}\right)^{\beta}\right)$$

where: α is relaxation strength; τ relaxation time; β stretch parameter. From the relaxation time, the diffusion rate and, consequently, the average radius value were obtained. The CONTIN analysis resulted in a size (diameter) distribution function. The CONTIN and KWW fitting were performed using Matlab R2014b.[39] It is worth to stress out that the CONTIN algorithm relies on inversed Laplace transform, which is a mathematically ill-posed problem. It means that there will be an infinite number of possible solutions.[40] We used the data from the KWW fitting as reference in the fitting process.

2.2.6. Small angle X-ray scattering (SAXS)

SAXS measurements were carried out with a HECUS S3-MICRO camera (Kratky-type) equipped with a position-sensitive detector (OED 50 M) containing 1024 channels of width 54 μm. Cu Kα radiation of wavelength λ = 1.542 Å was provided by an ultrabrilliant point microfocus X-ray source (GENIX-Fox 3D, Xenocs, Grenoble), operating at a maximum power of 50 W (50 kV and 1 mA). The sample-to-detector distance was 269 mm. Measurements were conducted under vacuum to minimize scattering from the air. The Kratky camera was calibrated in the small angle region using silver behenate (d = 58.38 Å).[41] Scattering curves were obtained in the q-range between 0.004 and 0.54 $Å^{-1}$, where q is the scattering vector, $q = 4\pi/\lambda \sin\theta$, and 2θthe scattering angle. The temperature control was set to 25 °C. Samples were contained in 1.5 mm thick quartz capillary tubes sealed with hot-melting glue. The concentration of samples was adjusted to 1–7 wt% using Milli-Q water. Desmearing of SAXS curves was not necessary thanks to the advanced focusing system. The low-q region of SAXS curves (0.04–0.01 $Å^{-1}$) was used to calculate the gyration radius (Rg). Rg can be obtained using the Guinier plot, in which Ln(I) is plotted against q^2. A linear fitting of the data gives the value of the slope, which is equal to $Rg^2/3$. The Guinier approximation holds for small angles ($q \times Rg < 1.7$).

2.2.7. Quartz crystal microbalance with dissipation monitoring (QCM-D)

QCM-D was used to measure adsorption at a model SiO_2 surfaces. The technique has been well described in the literature.[42,43] In brief, a piezoelectric quartz sensor crystal, in this case covered with SiO_2, oscillates at its resonance frequency under application of an electric field. This oscillation frequency is monitored at several overtones (3^{rd}, 5^{th}, 7^{th}, etc.) and depends on the mass of the crystals, which varies with adsorption. When the driving voltage is shut off, the oscillation decays exponentially with time, allowing the determination of a dissipation factor ΔD:

$$\Delta D = \frac{E_{dissipation}}{2\pi E_{stored}}$$

where $E_{dissipation}$ stands for loss in energy and E_{stored} is the stored energy of the adsorbed layer.

High value of ΔD usually indicates the presence of a viscoelastic film, which requires processing of the data using a model. In the present case we have used the Voigt model, which describes the propagation and damping of acoustic waves in a single undifferentiated viscoelastic adsorbed film in contact with a Newtonian bulk liquid. The frequency and dissipation variations from the 3rd, 5th and 7th overtone were used.[44,45]

Adsorption of polyelectrolytes on SiO_2 coated crystals was measured using a QCM-D E4 device (Q-sense AB, Göteborg, Sweden). The model surfaces were SiO_2 QCM-D crystals from Renlux, China. The crystal surfaces were cleaned in 10 wt% NaOH solution for 15 s, followed by rinsing with Milli-Q water and drying with nitrogen. Prior to any adsorption experiment, the crystals mounted in the QCM-D chamber were rinsed with water for 30 min, under a constant flow of 0.1 ml/min. Then the pH was adjusted first to 3, and the baseline was recorded. The PEI and CMC concentrations were 0.05 wt%. The measurements were conducted in 4 replicates, simultaneously, to ensure reproducibility.

The successive injection and pH adjustments were carried out in a similar fashion as for the PEM (polyelectrolyte multilayers) build-up approach on colloidal silica, under flow condition (0.1 ml/min), namely: (1) MilliQ water at pH 3, (2) 0.05 wt% PEI at pH 3, (3) 0.05 wt% PEI at pH 11, (4) MilliQ water at pH 11, (5) 0.05 wt% CMC at pH 10 (6) 0.05 wt% CMC at pH 3, (7) MilliQ water at pH 3. The pH was adjusted directly in the polyelectrolyte solution that was injected in the chamber to change it from 3 to 10 and vice-versa.

3. Results and discussion

Our PEM build-up strategy on silica nanoparticles is based on controlling the charge density of the components. Fig. 2 shows the charge density of the silica nanoparticles and of the two polyelectrolytes as function of pH, as determined by streaming potential titration. This procedure is based on monitoring the apparent charge of a given mass of material during titration with a strong polyelectrolyte with known charge density until neutrality is reached. It gives an indication of the amount needed to achieve charge balance, with respect to the mass of the materials, not to the specific surfaces. As can be seen, silica is only weakly negatively charged at pH 3, as also reported in the literature.[33] PEI, on the other hand, is strongly positively charged at low pH but almost non-charged at pH 11. CMC is negatively charged over the entire pH range studied, and the charge density increases with increasing pH. One may note that the charge density of the silica surface is orders of magnitude smaller than those of the two PEs. The results from the measurements of charge density as function of pH were used to estimate the amounts of the various components needed to achieve charge reversal upon adsorption.

The build-up of the PE multilayers (PEM) starts by ion-exchanging a 40 wt%, 20 nm silica sol to pH 3, yielding silica nanoparticles of low surface charge. The use of an ion exchange resin to reduce the pH is a way to keep the ionic strength of the dispersion low. At this low pH colloidal silica is metastable and will gel within a few days.[33,46,47] However, the dispersion is stable enough to perform the PEM strategy. PEI, which is strongly positively charged at this pH, was added without triggering flocculation. PEI can be either branched or linear, and the branched PEI was preferred for stability reasons. These results are in agreement with previous findings.[48] The amount of PEI used to provide overcharge of the silica was small, only 0.2 wt% of the silica, so as to avoid free polymer in the bulk phase. The presence of free cationic PE in the aqueous phase would be detrimental in the next step, where an anionic PE is added. When PEI is added as the last and outermost layer, a much higher amount is used (~9 wt% of the silica), in order to achieve good colloidal stability below pH 10.

Following PEI addition, the pH of the PEI@SNP(*1*) suspension was raised to 11, leading to the strong attachment of PEI on the silica surface. The adsorption behavior of the polyelectrolyte was evaluated by measurements on a flat silica surface using quartz crystal microbalance with dissipation monitoring (QCM-D). This approach of using a macroscopic model surface for deciphering

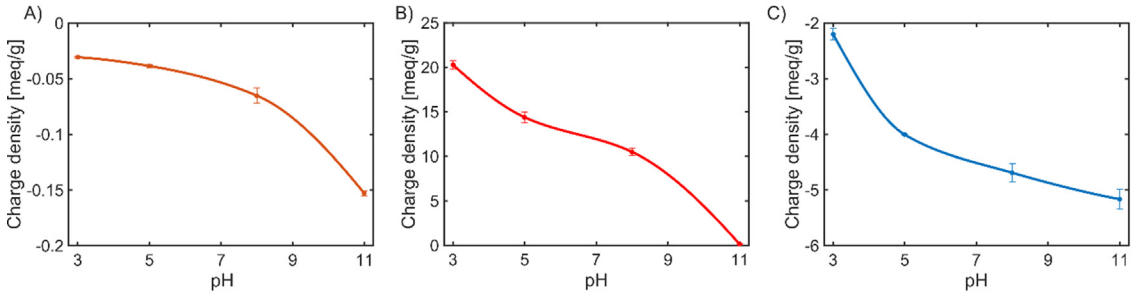

Fig. 2. Charge density of (A) SNP, (B) PEI and (C) CMC as function of pH. Solid lines are just guide for the eye. Titrations were done in triplicate.

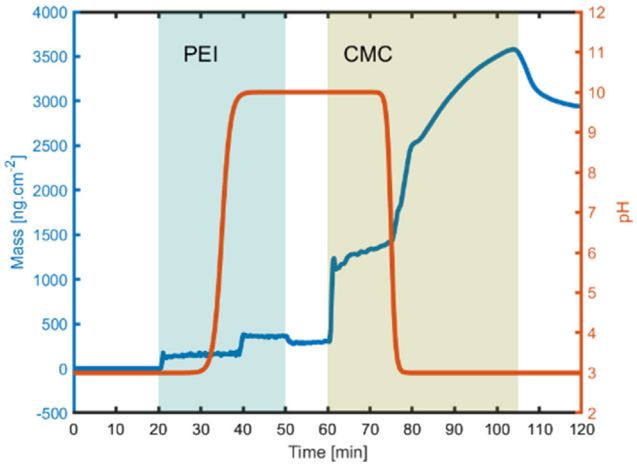

Fig. 3. Mass adsorbed during the PEM build-up process at a SiO_2 model surface monitored by QCM–D. The left axis refers to the mass uptake while the right axis describes the pH variation in the QCM–D measurement chamber. The colored regions indicate the period during which the SiO_2 surfaces were exposed to the different polyelectrolytes. Details regarding the data fitting are provided in Figures S1 and S2. Adsorption experiments were done in 4 replicates.

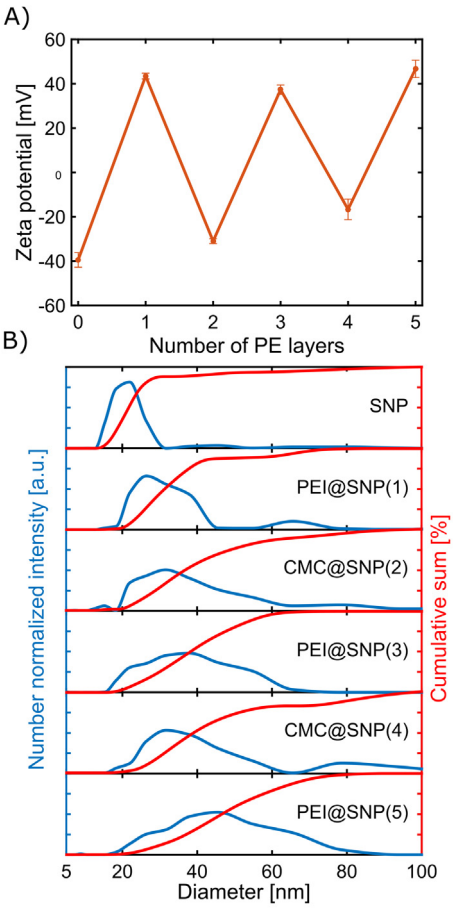

Fig. 4. (A) Zeta potential of PE-coated silica nanoparticles with varying number of PE layers. (B) Particle size distributions determined from DLS data using the CONTIN algorithm. The left y-axis shows intensity in arbitrary units and the right y-axis is the cumulative sum in percent. Measurements were done in triplicate, at a concentration of 0.05 wt%, in MilliQ water for DLS and in 2 mM NaCl for zeta potential measurements.

the mechanism of adsorption onto particle surfaces has previously proven to be useful.[49,50] Here, we used it to assess the adsorption of PEI and CMC at a silica surface over the relevant pH range (see Fig. 3). Above pH 10, CMC is negatively charged, and PEI@SNP(*1*) is almost non-charged. The amount of CMC added was equal to the amount of added PEI, i.e. 0.2 wt% of the silica. As with PEI, the amount of CMC added as the final layer was much higher, ~9 wt% of the silica. The adsorption of CMC triggered by the decrease of pH was also evidenced by the QCM-D experiment. Treatment with an ion exchange resin brought the pH back to 3 and another addition of PEI was made, etc. Dry mass and percentage content of each component are presented in Table S1. The pH range for which the samples exhibited stability over a period of 6 months is also given. Given the pH range in which the samples were stable, it is very likely that steric stabilization is also at play, while the main forces preventing aggregation are of electrostatic nature. Furthermore, the presence of a double layer of CMC-PEI was found to be beneficial for the stability within the relevant pH range, most likely because it ensured the presence of charges at the surface of the particles. This is a further indication of the importance of the electrostatic contribution to the mechanism of stabilization.

Zeta potential measurements were performed in order to track the charge reversal during adsorption of subsequent PE layers (Fig. 4A). The bare SNP had a zeta potential of − 40 mV, which changed to + 43 mV when PEI was adsorbed, indicating a strong overcharging. Such a high value is beneficial for the colloidal stability. In general, the zeta potential for the coated particles with PEI as the final layer was around + 42 mV, whereas for the particles with CMC as the final layer, the negative zeta potential values were reduced with increasing number of PE layers. This has been observed before for larger number of layers and has been attributed to interpenetration of the polyelectrolytes.[51]

The coated nanoparticles were characterized with DLS using the CONTIN algorithm for the analysis. To avoid misinterpretation of the experimental data, the fitting with CONTIN was always correlated with the average radius values obtained from a stretched exponential fit, even though this latter is known to be influenced

Table 1
Particle size as determined by SAXS analyses of the samples. Rg and Rh are the radius of gyration and the hydrodynamic radius, respectively. The experimental error for the Rh and Rg values is about 1%.

Sample	Rg [nm]	Rh [nm]	Rg/Rh
SNP	17.6	20.7	0.85
PEI@SNP(*1*)	18.1	30.2	0.60
CMC@SNP(*2*)	17.4	35.7	0.49
PEI@SNP(*3*)	18.2	37.2	0.49
CMC@SNP(*4*)	17.5	42.6	0.41
PEI@SNP(*5*)	18.0	44.9	0.40

by the polydispersity of the system (KWW function, see hydrodynamic radius, Rh, values in Table 1, and discussion in Supporting Material).[52] Fig. 4B shows the size analysis of the particles, along with the cumulative sum of intensity, as percentage value. The cumulative sum gives the fraction, in terms of scattering intensity contribution, to the total intensity of the sample. For SNP the main fraction lies between 15 nm and 30 nm in diameter and traces of bigger particles and/or small aggregates can be found in the diameter range 35–50 nm, accounting for 10% of the scattering intensity. After adsorption of the first PEI layer, the main fraction increases to the diameter range 20–45 nm, as expected for an added monolayer of branched PEI, where some minor aggregation could take place.[53] The analysis indicates that the main population consists of single particles coated with PEI; however, there is also a minor fraction of small aggregates consisting of up to 4 silica particles. The average diameter remained below 45 nm. Successive addition of polyelectrolytes yielded a continuous increase of the dimension of the particles. After addition of two layers the diameter was between 25 nm and 60 nm. There was also a small fraction with a diameter around 15 nm that may be attributed to a PEI-CMC complex. The last curve in Fig. 4B shows the size distribution of the particles with 5 PE layers and with PEI as the outermost coating. The distribution is broad and relatively symmetric, centered around a diameter of 50 nm. For reference, DLS was also performed on samples prepared from a much lower silica concentration, 0.5 wt% instead of 40 wt%. Figure S3 shows that the size distributions for PEI@SNP(*1*) and CMC@SNP(*2*) are similar to those prepared starting from the diluted silica dispersion.

The PE-coated silica nanoparticles were further characterized by SAXS (see Fig. 5 and Table 1). The samples displayed similar scattering profiles, regardless of the number of PE layers.

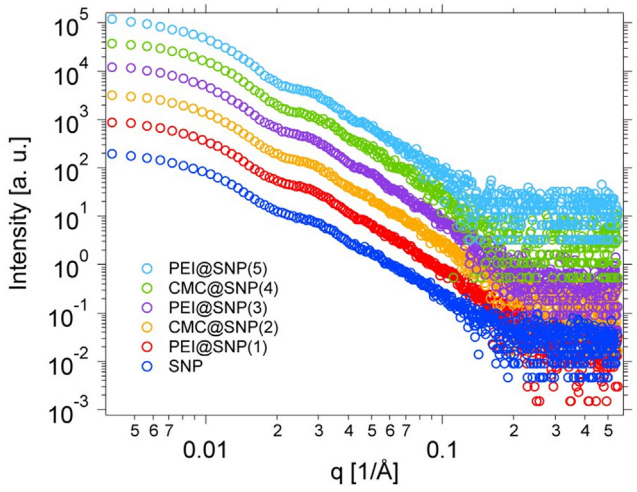

Fig. 5. SAXS curves of silica/PE complexes with different number of PE layers. The curves were arbitrarily offset, for sake of clarity.

The low-q region was used to calculate the gyration radius (Rg) using the Guinier approximation. The radius of gyration, Rg, of bare silica particles was 17.6 nm, which is in good agreement with previously reported values for the SNP.[54] The obtained Rg, and the Rg/Rh ratios, are presented in Table 1. The Rg/Rh ratio for the untreated particles was 0.85, close to the value of 0.77 that is characteristic for a hard sphere. The Rh values increased with an increasing number of PE layers, as can be seen from Table 1. On the other hand, the Rg of the coated silica particles were almost the same as the Rg of the bare silica particles, which means that the Rg/Rh ratio decreased with increasing number of PE layers. This variation of Rg and Rh values can be explained by the fact that the scattering length density of the PEI/CMC layers is almost identical to that of water, making the shell undetectable with SAXS. Similar findings have been reported elsewhere for related core–shell systems. These results support the view that the assembly process is well under control and that aggregates composed of silica particles are not formed.

4. Conclusions

The problem of aggregation during polyelectrolyte multilayers build-up has often constituted a major hindrance to reach large scale applications of colloidal systems, as it requires tedious washing steps or the use of low concentration of particles (<1 wt%). Addition of excess polymer is also problematic, as it often strongly interacts with the other, oppositely charged, polymer leading to formation of a polymer complex.[30,55,56]

Here we report an approach to assemble PE layers on silica, using stock nanoparticle concentrations as high as 40 wt%. In this approach, the key is the control of the charges of weak polyelectrolytes through pH, which allows separating mixing and adsorption events. Mixing is done at a pH where adsorption is not favored, thus preventing aggregation to occur. This step is followed by a change in pH in order to trigger adsorption. Salt build-up, that can lead to aggregation, is avoided by the use of ion-exchange resins.

Contrary to build-up conducted by spraying and other conventional methods,[57] sequential adsorption can be carried out, starting with concentrated suspension (40 wt%) to reach a final concentration of nanoparticles above 4 wt%. In practice, the cationic polymer, PEI, was adsorbed at low pH, at which silica is not charged, and the anionic polymer, CMC, was introduced at high pH, at which PEI is only slightly charged. Five PE layers were applied without any major change in size of the particles.

A multianalytical approach was followed to obtain a thorough and self-consistent picture of the obtained systems. In detail, DLS proved the deposition of PE though the increase of the hydrodynamic diameter with increasing number of layers. On the other hand, SAXS measurements showed that no aggregation occurred during PE deposition. Finally, QCM-D directly demonstrated that our approach allowed to build a multilayered PE structure on a model silica surface. Future perspectives might involve studies dedicated to the direct imaging of the particles, e.g. using Cryo-electron microscopy, or by etching out the particles to remove their core.

The developed procedure to perform layer-by-layer deposition of polyelectrolytes in a concentrated particle suspension is practically important as nanoparticles functionalized by polyelectrolyte multilayers is an ubiquitous technology that has proven its efficiency in many applications.[57] The results reported here eliminates one of the main constraints for industrial use by avoiding many of the purification and solvent evaporation steps needed to obtain suspensions of industrial relevance. The limitation now lies in the viscosity of the polymer stock solutions, which could

partially be addressed by tuning the structures and molecular weights of the polyelectrolytes, as well as considering alternative mixing approaches.

Declaration of Competing Interest

The authors declare that they have no known competing financial interests or personal relationships that could have appeared to influence the work reported in this paper.

Acknowledgement

This work has received funding from the European Union's Horizon 2020 research and innovation programme under the NanoRestArt project (Grant Agreement No. 646063).

Appendix A. Supplementary material

Supplementary data to this article can be found online at https://doi.org/10.1016/j.jcis.2022.01.120.

References

[1] A.C. Balazs, T. Emrick, T.P. Russell, Nanoparticle polymer composites: where two small worlds meet, Science 314 (5802) (2006) 1107–1110, https://doi.org/10.1126/science.1130557.
[2] J. Rieger, M. Kellermeier, L. Nicoleau, Formation of Nanoparticles and Nanostructures—An Industrial Perspective on CaCO3, Cement, and Polymers, Angew. Chemie Int. Ed. 53 (2014) 12380–12396, https://doi.org/10.1002/anie.201402890.
[3] F. Caruso, R.A. Caruso, H. Mőhwald, Nanoengineering of Inorganic and Hybrid Hollow Spheres by Colloidal Templating, Science 282 (5391) (1998) 1111–1114.
[4] Y. Yang, K. Achazi, Y.i. Jia, Q. Wei, R. Haag, J. Li, Complex Assembly of Polymer Conjugated Mesoporous Silica Nanoparticles for Intracellular pH-Responsive Drug Delivery, Langmuir. 32 (47) (2016) 12453–12460, https://doi.org/10.1021/acs.langmuir.6b01845.
[5] H.M.G. Barriga, M.N. Holme, M.M. Stevens, Cubosomes: The Next Generation of Smart Lipid Nanoparticles?, Angew Chemie Int. Ed. 58 (2019) 2958–2978, https://doi.org/10.1002/anie.201804067.
[6] C. Zhou, Z. Shen, L.-H. Liu, S. Liu, Preparation and functionality of clay-containing films, J. Mater. Chem. 21 (2011) 15132, https://doi.org/10.1039/c1jm11479d.
[7] F. Iselau, P. Restorp, M. Andersson, R. Bordes, Role of the aggregation behavior of hydrophobic particles in paper surface hydrophobation, Colloids Surfaces A Physicochem. Eng. Asp. 483 (2015) 264–270, https://doi.org/10.1016/j.colsurfa.2015.04.013.
[8] G. Poggi, N. Toccafondi, D. Chelazzi, P. Canton, R. Giorgi, P. Baglioni, Calcium hydroxide nanoparticles from solvothermal reaction for the deacidification of degraded waterlogged wood, J. Colloid Interface Sci. 473 (2016) 1–8, https://doi.org/10.1016/j.jcis.2016.03.038.
[9] G. Poggi, R. Giorgi, A. Mirabile, H. Xing, P. Baglioni, A stabilizer-free non-polar dispersion for the deacidification of contemporary art on paper, J. Cult. Herit. 26 (2017) 44–52, https://doi.org/10.1016/j.culher.2017.02.006.
[10] D. Chelazzi, G. Poggi, Y. Jaidar, N. Toccafondi, R. Giorgi, P. Baglioni, Hydroxide nanoparticles for cultural heritage: Consolidation and protection of wall paintings and carbonate materials, J. Colloid Interface Sci. 392 (2013) 42–49, https://doi.org/10.1016/J.JCIS.2012.09.069.
[11] K. Kolman, O. Nechyporchuk, M. Persson, K. Holmberg, R. Bordes, Combined Nanocellulose/Nanosilica Approach for Multiscale Consolidation of Painting Canvases, ACS Appl. Nano Mater. 1 (5) (2018) 2036–2040, https://doi.org/10.1021/acsanm.8b0026210.1021/acsanm.8b00262.s001.
[12] N. Palladino, M. Hacke, G. Poggi, O. Nechyporchuk, K. Kolman, Q. Xu, M. Persson, R. Giorgi, K. Holmberg, P. Baglioni, P. Baglioni, R. Bordes, Nanomaterials for combined stabilisation and deacidification of cellulosic materials—the case of iron-tannate dyed cotton, Nanomaterials. 10 (2020), https://doi.org/10.3390/nano10050900.
[13] P. Baglioni, D. Chelazzi, How Science Can Contribute to the Remedial Conservation of Cultural Heritage, Chem. – A Eur. J. 27 (42) (2021) 10798–10806, https://doi.org/10.1002/chem.202100675.
[14] P.J. Roth, P. Theato, Versatile Synthesis of Functional Gold Nanoparticles: Grafting Polymers From and Onto, Chem. Mater. 20 (2008) 1614–1621, https://doi.org/10.1021/cm702642e.
[15] G. Schneider, G. Decher, From Functional Core/Shell Nanoparticles Prepared via Layer-by-Layer Deposition to Empty Nanospheres, Nano Lett. 4 (10) (2004) 1833–1839, https://doi.org/10.1021/nl0490826.
[16] G. Decher, J.D. Hong, J. Schmitt, Buildup of ultrathin multilayer films by a self-assembly process: III, Consecutively alternating adsorption of anionic and cationic polyelectrolytes on charged surfaces, Thin Solid Films. 210–211 (1992) 831–835, https://doi.org/10.1016/0040-6090(92)90417-A.
[17] G. Decher, Fuzzy nanoassemblies: toward layered polymeric multicomposites, science 277 (5330) (1997) 1232–1237, https://doi.org/10.1126/science.277.5330.1232.
[18] G. Schneider, G. Decher, N. Nerambourg, R. Praho, M.H.V. Werts, M. Blanchard-Desce, Distance-dependent fluorescence quenching on gold nanoparticles ensheathed with layer-by-layer assembled polyelectrolytes, Nano Lett. 6 (3) (2006) 530–536, https://doi.org/10.1021/nl052441s10.1021/nl052441s.s001.
[19] A.T. Nagaraja, Y.-H. You, J.-W. Choi, J.-H. Hwang, K.E. Meissner, M.J. McShane, Layer-by-layer modification of high surface curvature nanoparticles with weak polyelectrolytes using a multiphase solvent precipitation process, J. Colloid Interface Sci. 466 (2016) 432–441, https://doi.org/10.1016/j.jcis.2015.12.040.
[20] J. Blaakmeer, M.R. Bohmer, M.A.C. Stuart, G.J. Fleer, Adsorption of weak polyelectrolytes on highly charged surfaces. Poly(acrylic acid) on polystyrene latex with strong cationic groups, Macromolecules. 23 (8) (1990) 2301–2309, https://doi.org/10.1021/ma00210a028.
[21] M. Borkovec, I. Szilagyi, I. Popa, M. Finessi, P. Sinha, P. Maroni, G. Papastavrou, Investigating forces between charged particles in the presence of oppositely charged polyelectrolytes with the multi-particle colloidal probe technique, Adv. Colloid Interface Sci. 179–182 (2012) 85–98, https://doi.org/10.1016/J.CIS.2012.06.005.
[22] F. Miano, M.R. Rabaioli, Rheological scaling of montmorillonite suspensions: the effect of electrolytes and polyelectrolytes, Colloids Surfaces A Physicochem. Eng. Asp. 84 (1994) 229–237, https://doi.org/10.1016/0927-7757(93)02724-S.
[23] N.G. Veerabadran, D. Mongayt, V. Torchilin, R.R. Price, Y.M. Lvov, Organized Shells on Clay Nanotubes for Controlled Release of Macromolecules, Macromol. Rapid Commun. 30 (2) (2009) 99–103, https://doi.org/10.1002/marc.200800510.
[24] S. Såringer, P. Rouster, I. Szilagyi, Co-immobilization of antioxidant enzymes on titania nanosheets for reduction of oxidative stress in colloid systems, J. Colloid Interface Sci. 590 (2021) 28–37, https://doi.org/10.1016/J.JCIS.2021.01.012.
[25] Y. Zhu, J. Shi, W. Shen, X. Dong, J. Feng, M. Ruan, Y. Li, Stimuli-Responsive Controlled Drug Release from a Hollow Mesoporous Silica Sphere/Polyelectrolyte Multilayer Core-Shell Structure, Angew, Chemie. 117 (32) (2005) 5213–5217, https://doi.org/10.1002/ange.200501500.
[26] A. Tiraferri, P. Maroni, M. Borkovec, Adsorption of polyelectrolytes to like-charged substrates induced by multivalent counterions as exemplified by poly (styrene sulfonate) and silica, Phys. Chem. Chem. Phys. 17 (16) (2015) 10348–10352, https://doi.org/10.1039/C5CP00910C.
[27] M. Borkovec, G. Papastavrou, Interactions between solid surfaces with adsorbed polyelectrolytes of opposite charge, Curr. Opin. Colloid Interface Sci. 13 (6) (2008) 429–437, https://doi.org/10.1016/j.cocis.2008.02.006.
[28] S.E. Burke, C.J. Barrett, Acid−Base Equilibria of Weak Polyelectrolytes in Multilayer Thin Films, Langmuir. 19 (8) (2003) 3297–3303, https://doi.org/10.1021/la026500i.
[29] G.M. Lindquist, R.A. Stratton, The role of polyelectrolyte charge density and molecular weight on the adsorption and flocculation of colloidal silica with polyethylenimine, J. Colloid Interface Sci. 55 (1) (1976) 45–59, https://doi.org/10.1016/0021-9797(76)90007-2.
[30] N.G. Hoogeveen, M.A. Cohen Stuart, G.J. Fleer, M.R. Böhmer, Formation and Stability of Multilayers of Polyelectrolytes, Langmuir. 12 (15) (1996) 3675–3681, https://doi.org/10.1021/la951574y.
[31] K. Ariga, Y. Lvov, M. Onda, I. Ichinose, T. Kunitake, Alternately Assembled Ultrathin Film of Silica Nanoparticles and Linear Polycations, Chem. Lett. 26 (2) (1997) 125–126, https://doi.org/10.1246/cl.1997.125.
[32] Y. Shin, J.E. Roberts, M.M. Santore, The Relationship between Polymer/Substrate Charge Density and Charge Overcompensation by Adsorbed Polyelectrolyte Layers, J. Colloid Interface Sci. 247 (1) (2002) 220–230.
[33] R.K. Iler, The chemistry of silica : solubility, polymerization, colloid and surface properties, and biochemistry, Wiley, 1979.
[34] R. Wäsche, M. Naito, V.A. Hackley, Experimental study on zeta potential and streaming potential of advanced ceramic powders, Powder Technol. 123 (2-3) (2002) 275–281, https://doi.org/10.1016/S0032-5910(01)00462-4.
[35] K. Böckenhoff, W. Fischer, Determination of electrokinetic charge with a particle-charge detector, and its relationship to the total charge, Fresenius, J. Anal. Chem. 371 (5) (2001) 670–674, https://doi.org/10.1007/s002160100897.
[36] R.J. Hunter, The Calculation of Zeta Potential, Zeta Potential Colloid Sci. (1981) 59–124, https://doi.org/10.1016/B978-0-12-361961-7.50007-9.
[37] S.W. Provencher, A constrained regularization method for inverting data represented by linear algebraic or integral equations, Comput. Phys. Commun. 27 (3) (1982) 213–227, https://doi.org/10.1016/0010-4655(82)90173-4.
[38] S.W. Provencher, CONTIN: A general purpose constrained regularization program for inverting noisy linear algebraic and integral equations, Comput. Phys. Commun. 27 (1982) 229–242, https://doi.org/10.1016/0010-4655(82)90174-6.
[39] I.-G. Marino, Regularized Inverse Laplace Transform (RILT) - MatLab Script, (2007).
[40] A. Scotti, W. Liu, J.S. Hyatt, E.S. Herman, H.S. Choi, J.W. Kim, L.A. Lyon, U. Gasser, A. Fernandez-Nieves, The CONTIN algorithm and its application to determine the size distribution of microgel suspensions, J. Chem. Phys. 142 (2015), https://doi.org/10.1063/1.4921686 234905.

[41] T.N. Blanton, T.C. Huang, H. Toraya, C.R. Hubbard, S.B. Robie, D. Louer, H.E. Göbel, G. Will, R. Gilles, T. Raftery, JCPDS—International Centre for Diffraction Data round robin study of silver behenate. A possible low-angle X-ray diffraction calibration standard, Powder Diffr. 10 (2) (1995) 91–95, https://doi.org/10.1017/S0885715600014421.
[42] F. Höök, M. Rodahl, P. Brzezinski, B. Kasemo, Energy Dissipation Kinetics for Protein and Antibody−Antigen Adsorption under Shear Oscillation on a Quartz Crystal Microbalance, Langmuir. 14 (4) (1998) 729–734, https://doi.org/10.1021/la970815u.
[43] M. Rodahl, B. Kasemo, A simple setup to simultaneously measure the resonant frequency and the absolute dissipation factor of a quartz crystal microbalance, Rev. Sci. Instrum. 67 (9) (1996) 3238–3241, https://doi.org/10.1063/1.1147494.
[44] F. Höök, B. Kasemo, T. Nylander, C. Fant, K. Sott, H. Elwing, Variations in Coupled Water, Viscoelastic Properties, and Film Thickness of a Mefp-1 Protein Film during Adsorption and Cross-Linking: A Quartz Crystal Microbalance with Dissipation Monitoring, Ellipsometry, and Surface Plasmon Resonance Study, Anal. Chem. 73 (2001) 5796–5804, https://doi.org/10.1021/ac0106501.
[45] M.V. Voinova, M. Rodahl, M. Jonson, B. Kasemo, Viscoelastic Acoustic Response of Layered Polymer Films at Fluid-Solid Interfaces: Continuum Mechanics Approach, Phys. Scr. 59 (1999) 391–396, https://doi.org/10.1238/physica.regular.059a00391.
[46] J.J. Adler, Y.I. Rabinovich, B.M. Moudgil, Origins of the Non-DLVO Force between Glass Surfaces in Aqueous Solution, J. Colloid Interface Sci. 237 (2) (2001) 249–258, https://doi.org/10.1006/jcis.2001.7466.
[47] M. Kobayashi, M. Skarba, P. Galletto, D. Cakara, M. Borkovec, Effects of heat treatment on the aggregation and charging of Stöber-type silica, J. Colloid Interface Sci. 292 (1) (2005) 139–147, https://doi.org/10.1016/j.jcis.2005.05.093.
[48] J.F. Bringley, A. Wunder, A.M. Howe, R.D. Wesley, T.A. Qiao, N.B. Liebert, B. Kelley, J. Minter, B. Antalek, J.M. Hewitt, Controlled, simultaneous assembly of polyethylenimine onto nanoparticle silica colloids, Langmuir. 22 (9) (2006) 4198–4207, https://doi.org/10.1021/la0534118.
[49] Q. Chen, S. Xu, Q. Liu, J. Masliyah, Z. Xu, QCM-D study of nanoparticle interactions, Adv. Colloid Interface Sci. 233 (2016) 94–114, https://doi.org/10.1016/J.CIS.2015.10.004.
[50] J. Engström, M.S. Reid, E.E. Brotherton, E. Malmström, S.P. Armes, F.L. Hatton, Investigating the adsorption of anisotropic diblock copolymer worms onto planar silica and nanocellulose surfaces using a quartz crystal microbalance, Polym. Chem. 12 (42) (2021) 6088–6100, https://doi.org/10.1039/D1PY00644D.
[51] R.A. Ghostine, M.Z. Markarian, J.B. Schlenoff, Asymmetric Growth in Polyelectrolyte Multilayers, J. Am. Chem. Soc. 135 (20) (2013) 7636–7646, https://doi.org/10.1021/ja401318m.
[52] C.-N. Lin, Y.-M. Song, T.-L. Yu, Dynamic light scattering and viscoelasticity of semidilute polystyrene/cyclohexane solutions, J. Polym. Res. 4 (2) (1997) 107–117, https://doi.org/10.1007/s10965-006-0014-2.
[53] M. Schönhoff, Self-assembled polyelectrolyte multilayers, Curr. Opin. Colloid Interface Sci. 8 (1) (2003) 86–95, https://doi.org/10.1016/S1359-0294(03)00003-7.
[54] A. Lamberty, K. Franks, A. Braun, V. Kestens, G. Roebben, T.P.J. Linsinger, Interlaboratory comparison for the measurement of particle size and zeta potential of silica nanoparticles in an aqueous suspension, J. Nanoparticle Res. 13 (12) (2011) 7317–7329, https://doi.org/10.1007/s11051-011-0624-4.
[55] E. Donath, D. Walther, V.N. Shilov, E. Knippel, A. Budde, K. Lowack, C.A. Helm, H. Möhwald, Nonlinear Hairy Layer Theory of Electrophoretic Fingerprinting Applied to Consecutive Layer by Layer Polyelectrolyte Adsorption onto Charged Polystyrene Latex Particles, Langmuir. 13 (20) (1997) 5294–5305, https://doi.org/10.1021/la970090u.
[56] G.B. Sukhorukov, E. Donath, H. Lichtenfeld, E. Knippel, M. Knippel, A. Budde, H. Möhwald, Layer-by-layer self assembly of polyelectrolytes on colloidal particles, Colloids Surfaces A Physicochem. Eng. Asp. 137 (1-3) (1998) 253–266, https://doi.org/10.1016/S0927-7757(98)00213-1.
[57] J.J. Richardson, J. Cui, M. Björnmalm, J.A. Braunger, H. Ejima, F. Caruso, Innovation in Layer-by-Layer Assembly, Chem. Rev. 116 (23) (2016) 14828–14867, https://doi.org/10.1021/acs.chemrev.6b00627.